Applied Catalysis B: Environmental 145 (2014) 167–176

Contents lists available at ScienceDirect

Applied Catalysis B: Environmental

journal homepage: www.elsevier.com/locate/apcatb

Catalytic hydroconversion of a wheat straw soda lignin: Characterization of the products and the lignin residue

B. Joffres[a,b], C. Lorentz[a], M. Vidalie[b], D. Laurenti[a,*], A.-A. Quoineaud[b], N. Charon[b], A. Daudin[b], A. Quignard[b], C. Geantet[a]

[a] Institut de Recherches sur la Catalyse et l'Environnement de Lyon, IRCELYON, UMR 5256, CNRS-Université de Lyon 1, 2 avenue Albert Einstein, 69626 Villeurbanne cedex, France
[b] IFP Energies Nouvelles, Rond point de l'échangeur de Solaize, BP3, 69360 Solaize, France

ARTICLE INFO

Article history:
Available online 29 January 2013

Keywords:
Conversion
Lignin
Hydroliquefaction
H-donor solvent, $NiMo/Al_2O_3$
Lignin residue
Bio-liquid

ABSTRACT

A wheat straw soda lignin was characterized and converted into gases and liquids under H_2 pressure, at 350 °C over a supported NiMo sulfide catalyst, using tetralin as a hydrogen-donor solvent in a batch autoclave. The aim of this work was to evaluate the transformations occurring during the temperature increasing step to reach a pseudo-t_0 and the impact of the catalyst presence in the mixture. A well-developed products separation protocol made possible to isolate and to characterize gases, organic liquid, lignin residue and solids (catalyst and char). A limited quantity of solids (or char) was produced however. As the lignin residue is one of the main intermediates of the lignin conversion pattern, the nature of this material has to be carefully determined. Thanks to several appropriate characterization techniques (GPC, NMR, FTIR), the conversion was followed and the lignin residue was compared to the initial lignin in order to understand the transformations occurring during the process.

1. Introduction

Nowadays valorization of lignin represents a real challenge as every year, more than 50 millions of tons of lignin are co-produced from pulp industry and burned to provide energy in this field of activity. However, a part of this lignin could be used for other applications without weakening the pulp industry. In addition, the improvement of the pulping processes and new patented processes toward very pure sulfur-free lignins should provide even greater quantities of quality material [1–3]. Furthermore, in the perspective of an intensive cellulosic ethanol production as biofuel by the enzymatic route, the lignin resources could dramatically increase in a near future [4].

The use of lignin as a precursor of carbonaceous materials has gained interest due to its low cost and high availability. One way of valorization is based on the production of chemicals like phenols or aromatics (BTX: Benzene Toluene Xylene) from the polyphenolic structure. However, routes of valorization need to be improved [5–9]. The difficulty of the valorization of the lignin comes from its complex polymeric structure which differs from one lignin to another depending on the botanical origin and on the pretreatment used for its separation from carbohydrates (cellulose and hemicellulose). All lignins are mainly build up by the combination of three hydroxyl-phenylpropane units differently substituted [10] and interlinked by C—O or C—C bonds. The principal linkage of raw lignins is the ether linkage β-O-4 which is easily cleaved during delignification processes. Moreover β–β, β-O-5, 5–5′, spirodienone, dibenzodioxocin, and phenylcoumaran linkages can be present (Fig. 1) in various ratios depending of the origin of the lignin [11].

The most common pulping processes are the alkaline kraft or soda processes that involve alkaline solutions of NaSH or NaOH used at medium temperature (150–170 °C) to solubilize lignin from biomass while cellulosic material stays in the solid state and can be recovered by filtration. In this kind of process the lignin structure is more or less transformed. For instance, reduction reactions like cleavage of β-aryl linkage in β-O-4 structures may occur during kraft pulping [12]. The sulfite process is generally undertaken with pH varying between 2 and 12 at 125–150 °C in the presence of calcium or magnesium sulfite reagents. By this way, sulfonic acid groups are introduced in the lignin structure and the lignosulfonates obtained are used in different types of applications such as pigments, emulsifiers or adhesives [10]. Other fractionating processes like organosolv (using organic solvents) allow isolating sulfur-free lignin generally after a mechanical pre-treatment [13,14]. Finally, the biomass steam explosion process gives access to higher molecular weight lignins compared to all the other processes [14]. This process used for the saccharification of lignocelluloses for glucose and ethanol production [15] could become an important process in the future and a significant new lignin resource.

* Corresponding author. Tel.: +33 04 72445327; fax: +33 04 72445399.
E-mail address: dorothee.laurenti@ircelyon.univ-lyon1.fr (D. Laurenti).

0926-3373/$ – see front matter © 2013 Elsevier B.V. All rights reserved.
http://dx.doi.org/10.1016/j.apcatb.2013.01.039

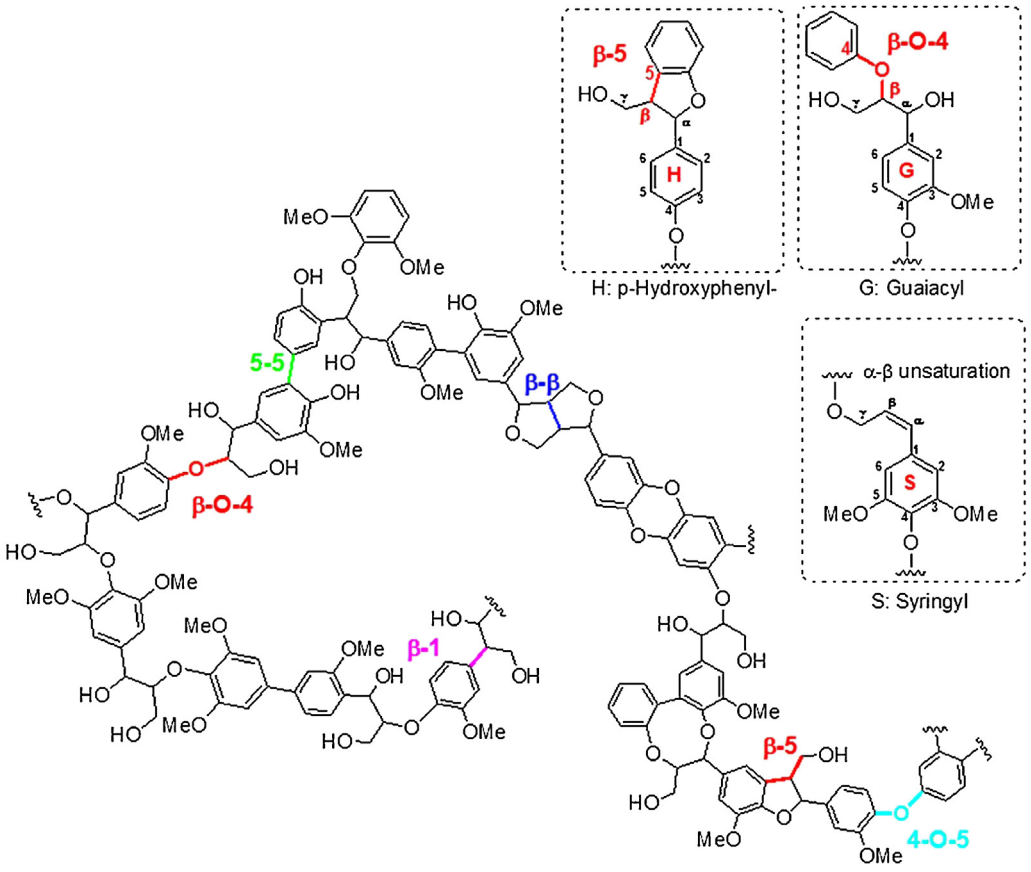

Fig. 1. Principal linkages and functional groups in soda lignin.

Like other types of biomass, the solid lignin material can be converted into liquids by thermochemical transformations. Among the different processes proposed in the literature, the direct liquefaction under hydrogen pressure using a catalyst, or hydroliquefaction, was proposed as a promising way as compared to pyrolysis which lead mostly to gases and char and offer lower liquid yields (40–60 wt%) [16–20]. Furthermore, the thermochemical conversion of lignin using hydrotreating catalysts with an H-donor solvent and/or with hydrogen at relatively high pressure, as previously developed for the coal liquefaction [21–23], was described as the best way to obtain high liquid yield with low quantity of char and partially deoxygenated from lignin [24–30]. Besides providing hydrogen in the liquid phase, the role of the H-donor solvent is also to stabilize the radical species coming from lignin degradation [31].

In this work we first present the characterization of the wheat straw lignin used (Protobind 1000). We then describe the experimental protocol as well as the separation and the characterization of hydroconversion products (i.e. gas, liquid, lignin residue and solid). Analytical methods such as CHONS elemental analysis, gel permeation chromatography (GPC), nuclear magnetic resonance (NMR), Fourier transform infrared (FTIR) spectroscopy and two-dimensional gas chromatography (GC × GC) were employed to clarify the conversion pathways and to propose a general reaction scheme.

2. Experimental

2.1. Materials and samples

2.1.1. Lignin

Protobind 1000 lignin was produced by soda pulping of a wheat straw and was supplied by Green Value (Switzerland).

2.1.2. Chemicals

The reagents used were 1,2,3,4-tetrahydronaphthalene (tetralin) (Sigma–Aldrich, ReagentPlus®, 99%), acetone (Sigma–Aldrich, CHROMASOLV®, for HPLC, ≥99.9%), dimethyldisulfide (Sigma–Aldrich, ≥99.0%), pyridine (Carlo Erba, purum, ≥99.9%), acetic anhydride (Prolabo, analytical grade), tetrahydrofuran (Sigma–Aldrich, analytical grade, ≥99.9%), *n*-heptane (Carlo-Erba, 99.2% pure) and 2-chloro-4,4,5,5-tetramethyl-1,3,2-dioxaphospholane (Sigma–Aldrich, 95%), $CDCl_3$ (Sigma–Aldrich, 99.8% atom D), DMSO-d_6 (Sigma–Aldrich, 99.9% atom D). The compounds used as reference compounds for product identification by gas chromatography (hydrogen, carbon monoxide, carbon dioxide, methane, ethane, propane, *n*-butane, isobutene, pentane, isopentane, hexane, 2-methylpentane, ethylene, propylene, 1-butene, 1,3-butadiene, 1-pentene, 1-hexene) were of analytical grade. The chemicals were used as received.

2.1.3. Catalyst

The catalyst was a NiMo catalyst supported over γ-alumina (shaped as extrudates), supplied by IFP Energies nouvelles (Solaize, France). This catalyst was obtained by incipient wetness impregnation as reported in a previous work [32], composed of NiO (3 wt%), MoO_3 (16 wt%) and P_2O_5 (6 wt%) and the BET surface area was 181 m^2/g.

2.2. Analytical methods

2.2.1. Elemental analyses

For C, H, O, N and S content measurements, a Thermo Scientific Flash 2000 apparatus was used. Oxygen was measured after pyrolysis by quantification of CO by a thermal conductivity detector. Carbon, hydrogen, nitrogen and sulfur were measured after

combustion and separation of CO_2, H_2O, SO_2 and NO_x, and quantification of these gases by a thermal conductivity detector. Other elemental analyses (metals) were performed by ICP-AES after solubilization of samples in acidic solutions using an Activa apparatus from Horiba Jobin Yvon.

2.2.2. Thermogravimetric analysis (TGA)

The lignin was thermally characterized by TGA with a SETARAM TGA 92 featuring automated temperature and weight control and data acquisition. The samples were analyzed as received using a heating rate of 5 °C/min from 25 to 800 °C. Air was used as carrier gas. The water content corresponds to the weight loss at 100 °C whereas the remaining weight at the end corresponds to the ash content.

2.2.3. Acetylation

The original lignin sample was acetylated prior to carry out gel permeation chromatography (GPC) analyses using tetrahydrofuran (THF) as eluent. This acetylation step allowed the complete solubilization of lignin in THF, as only 80 wt% of the lignin is soluble initially. Before acetylation, the lignin was dried at 60 °C under vacuum for 1 h and then 0.5 g was introduced in 25 mL of an equivalent volume of acetic anhydride and pyridine under argon. After 24 h of reaction, the reaction was stopped by adding 2 mL of cold distilled water. Then, the acetylated lignin was recovered with a dichloromethane extraction. The organic phase was then washed successively with a 100 mL NaCl saturated water and with 100 mL distilled water solution before co-evaporating the dichloromethane with toluene to recover the acetylated lignin.

2.2.4. Gel permeation chromatography (GPC)

GPC analyses were based on previously developed methods for lignin molecular weight determination [33–35]. Analyses were performed by using an Agilent apparatus (1200 series) equipped with two PLgel columns (50 and 500 Å) and a differential refractive index (DRI) detector. Analyses were carried out at 35 °C using THF as eluent at a flow rate of 1 mL/min. Samples were dissolved at around 5 wt% in THF before injection. The GPC system was calibrated with polystyrene standards in a molecular weight range from 162 to 55,100 g mol^{-1}. Depicted chromatograms were normalized to the sample weight. The lignin residues obtained after each hydroconversion run were completely soluble in THF and did not need to be acetylated.

2.2.5. Fourier transform-infrared spectroscopy

FTIR analyses were carried out in a transmission mode using a Vector 22 apparatus on Protobind 1000 lignin and lignin residues in order to get structural information. Pellets were prepared mixing 10 mg of samples in 150 mg of KBr. The range of data acquisition ran from 400 to 4000 cm^{-1} with a 0.96 cm^{-1} step.

2.2.6. Phosphorus NMR

^{31}P NMR technique was used for the characterization and the quantification of OH groups on the basis of previously developed methods involving a prior derivative phosphitylation step [36–38]. Samples were accurately weighted (c.a. 30 mg) and dissolved in a solution containing 200 mg of pyridine, 100 mg of an internal standard solution in pyridine (cyclohexanol, 15.7 mg/g), 100 mg of 2-chloro-4,4,5,5-tetramethyl-1,3,2-dioxaphospholane, and 200 mg of $CDCl_3$. ^{31}P NMR data were obtained with a Bruker Avance (250 MHz (^1H) 75 MHz (^{13}C)) probe QNP (Quad Nucleus Probe) 5 mm. The phosphorous atoms bonded to former alcohol or phenols have different chemical shifts that enable us to quantify each OH group.

2.2.7. Proton, carbon and heteronuclear single quantum coherence (HSQC) NMR

The 1D ^1H, ^{13}C NMR techniques enable basic structural characterizations. Around 50 mg of sample was dissolved in 700 mg of DMSO-d_6 using a Bruker Avance (250 MHz (^1H) 75 MHz (^{13}C)) probe QNP (Quad Nucleus Probe) 5 mm and Topspin 2.1 Bruker Software. ^1H spectra were acquired with single pulse acquisitions, ^{13}C spectra with inverse gated decoupling.

HSQC experiments allow identification of lignin structural units and the inter-unit patterns. The 2D HSQC were obtained on a Bruker Avance (600 MHz (^1H) 150.9 MHz (^{13}C)) probe BBI (Broadband inverse) 5 mm and Topspin 2.1 Bruker Software. The HSQC pulse sequence is based on proton and carbon bonding via J^1_{C-H} coupling constants. All the acquisitions were done by heating the samples at 50 °C. Due to broad and overlapping signals only relative quantifications were obtained by ^1H and ^{13}C NMR while ^{31}P NMR allowed absolute quantification thanks to the use of an internal standard.

2.2.8. μGC–TCD–MS

The μGC–TCD–MS technique was used to characterize gases formed during lignin hydroconversion. They were recovered in tedlar bags after cooling down the reactor at room temperature and compounds were separated with a μGC (SRA) equipped with three columns and coupled with a MS (Agilent 5975C). A 5 Å molecular sieve column (10 m, 12 μm) was used to analyze H_2, CH_4 and CO; the carrier gas was argon; the backflush injector temperature was maintained at 80 °C and column temperature was kept constant at 90 °C. A Poraplot U column (8 m, 30 μm) was used to separate CO_2, ethane, ethylene and H_2S; the carrier gas was hydrogen; the backflush injector temperature was maintained at 90 °C and column temperature was kept constant at 80 °C. An alumina column (10 m, 3 μm) was used to analyze C_3–C_6 hydrocarbons; the gas carrier was hydrogen; injection temperature was maintained at 100 °C, while column temperature was kept constant at 90 °C. Two detectors were used: a mass spectrometer for identification and a TCD detector for quantification.

2.2.9. GC × GC–MS

GC × GC chromatograms were recorded using an Agilent 6890 apparatus with a liquid nitrogen cryogenic jet modulation from Zoex Corporation coupled with a 5975B qMS (scan parameters: from 45 to 300 u at 22 scan/s) detector. The first column was a non-polar ZB1 column (30 m × 0.25 mm × 0.25 μm) and the second column was a polar ZB50 column (2 m × 0.1 mm × 0.1 μm). The temperature program of the first oven started at 50 °C for 5 min and then was heated up at 2 °C/min until 310 °C. The second oven started at 50 °C for 0 min and then heated up at 2.3 °C/min until 200 °C and at 1.8 °C/min until 320 °C. The modulation time was 12 s. The NIST-MS 2011 database was used for blob identification. Samples were injected without any prior dilution.

2.3. Hydroliquefaction experiments

Hydroliquefaction experiments were undertaken in a 0.3 L batch reactor equipped with a 2 L H_2 ballast. 30 g of lignin (dried at 60 °C under vacuum for 1 h) was introduced in 70 g of tetralin (H-donor solvent) with 3 g of catalyst $NiMo/Al_2O_3$ and 16 μL of DMDS. DMDS was added to maintain the sulfidation state of the catalyst since the sulfur content of the feedstock was at a relatively low level, resulting in low H_2S partial pressure in the reactor. The DMDS contribution in the production of methane and H_2S has been removed from the produced gases distribution. Before each test, the catalyst was freshly sulfided ex situ under a flow of H_2S/H_2 (15/85 mol%) for 4 h at 400 °C (4 L h^{-1}).

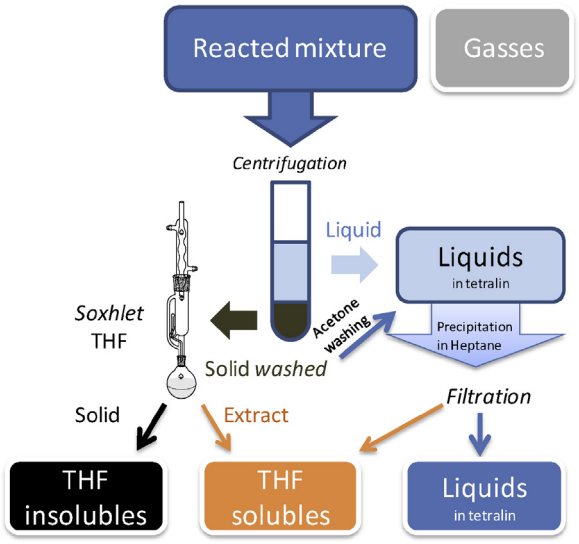

Fig. 2. Experimental protocol for the treatment of the reacted mixture.

The reactor was closed and flushed 3 times with 2.0 MPa of H_2. Finally 3.7 MPa of H_2 was introduced. Then, the reactor was heated up and stirring (800 rpm) was started. As soon as the reaction temperature (350 °C) was reached (14 min), H_2 was added to get 8 MPa and the ballast was opened to maintain this total pressure during all the experiment. One of the experiments was stopped as soon as the reaction temperature (350 °C) was reached in order to get a so-called t_0 point and to take into account the conversion due to the initial heating slope. Otherwise, after a residence time of 5 h, the run was stopped and the bottom of the reactor was cooled with an ice bath, while the top of the reactor was heated at 200 °C for 2 h to remove moisture deposition at the top of the reactor. By using this cooling down procedure, all the volatile products in the head of the reactor were recovered and the mass balance reached up to 98 wt% (±3.5 wt%). Without such a procedure, the mass balance was between 66 and 85 wt%. Before opening the reactor, the gases were collected in 5 L tedlar bags and analyzed with μGC–TCD–MS apparatus. Then, the quantification was obtained by using the gas reactor volume experimentally determined.

As described in Fig. 2, the reacted mixture was then centrifugated to isolate liquids and solids. The solids (including catalyst) were washed with acetone and further extracted in a Soxhlet apparatus using THF. After this step, the extrudate catalyst is thus separated from the other solids and further washed with heptane. The remaining solids were called "THF-insolubles fraction". The THF-solubles fraction was recovered after THF evaporation and a washing step was performed in the Soxhlet apparatus with heptane. The acetone contained in the liquid fraction recovered after the first washing of solids was evaporated and the remaining liquid was added to the liquid phase. The lignin residue is found either in the THF-solubles or THF-insolubles, however, the main fraction containing the lignin residue is the THF-solubles. The part of lignin residue in THF-insolubles will be called solid lignin residue. In the given yields, the ashes content was systematically subtracted.

In the liquid phase, which includes the tetralin solvent, we observed the presence of a certain amount of lignin-type residue which precipitates over the time. Therefore, we have developed a procedure to quantify this solid fraction: an experimentally determined heptane-to-liquid phase mass ratio of 7/10 was added to the liquid fraction to recover the residual lignin eventually solubilized in the liquid fraction by precipitation. After filtration and drying, the solid precipitate mass is added to the THF-solubles for the estimation of the conversion. The heptane precipitate was analyzed by GPC and the distribution, given in Supplementary material (Fig. S2), was found to be narrower but still close to the distribution of the THF-solubles fraction (lignin residue), then we deduced that the nature of these species was very similar to the lignin residue. The comparison of the GPC curves indicated that the heptane precipitate is a shorter lignin residue, which could explain its higher solubility in liquids.

Table 1
Elemental analysis of P1000 lignin and lignin residue after t_0 and after 5 h conversion without and with catalyst.

wt%	Lignin Protobind 1000	Lignin residue		
		t_0	5 h without catalyst	5 h with catalyst
C	59.4	70.7	76.1	80.0
H	5.6	5.8	4.9	6.5
O	25.7	22.0	12.4	11.3
N	1.1	1.3	2.4	2.4
S	0.1	0.0	0.1	0.0
Ashes	4.9	n.d.	n.d.	n.d.
Water	3.0	n.d.	n.d.	n.d.
Atomic ratios				
H/C	1.1	1.0	0.8	1.0
O/C	0.3	0.2	0.1	0.1

For all the runs, the ash-free conversion was defined as the ash free lignin conversion to liquids and gases, calculated according to the following equation:

$$\text{Conversion}\,(\%) = \left(1 - \frac{w(\text{THF-insolubles}) + w(\text{THF-solubles})}{w(\text{initial lignin-ash})}\right) \times 100$$

where w(THF-insolubles) is the mass of the solids obtained in the Soxhlet cartridge without the catalyst, w(THF-solubles) is the mass of solids recovered after THF evaporation and heptane precipitate from the liquid products, w(initial lignin-ash) is the initial mass of lignin used, subtracted of the mass of ashes found in the initial lignin.

In fact, the lignin residue was still considered as initial lignin which is not exactly the case, but this allows to avoid overestimation of the conversion. Thus, the conversion is not at all dissolution but formation of monomers, dimers, alkanes and gases.

3. Results and discussion

3.1. Characterization of Protobind 1000 lignin

The characterization of different lignins is well reported in the literature. In general, the C/H, and O/C atomic ratios, the syringyl/guaiacyl/p-hydroxyphenyl ratios (S/G/H), the ash and water content as well as the molecular weights distribution are described. These characterizations are, at least, required to follow the conversion of the lignin in thermochemical processes [39]. Moreover, in depth characterizations of chemical functions can be achieved by spectroscopic methods such as FTIR, or 1D and 2D NMR.

Elemental CHONS analyses, ash and water content as well as the H/C and O/C atomic ratios of Protobind 1000 lignin (P1000) are reported in Table 1. Water and ash content (at 600 °C) were determined by TGA (Supplementary material, Fig. S1) and were respectively equal to 3.0 and 4.9 wt% of the lignin. The ICP analysis of the ashes was carried out on the main metals previously detected by scanning electron microscopy (Supplementary material, Table S1).

The FTIR spectrum of the P1000 lignin shows the typical organic functions vibrations usually reported for lignin structures (HO—C_{ar}, HO—C_{al}, C_{ar}—OR, —OCH_3···) (Fig. 3 and Table S2) [40]. Syringyl and guaiacyl groups can be distinguished by C_{ar}—O—C bond (respectively 1334 cm^{-1} and 1183 cm^{-1}), and C_{ar}—H bond

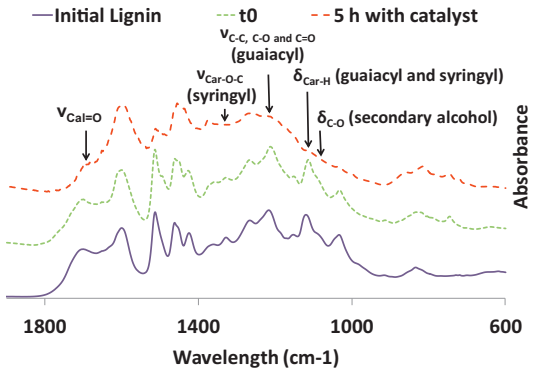

Fig. 3. FTIR spectra of P1000 lignin and lignin residues at t_0 and t = 5 h.

(respectively 1125 cm^{-1} and 838 cm^{-1}). In addition, aliphatic OH (1090 cm^{-1}) and non-conjugated C=O (1700–1715 cm^{-1}) vibrations were observed, the last one could be attributed to the presence of carboxylic acids on aliphatic chains or to remaining wheat triglycerides (esters) in the P1000 lignin.

^{1}H, ^{13}C and ^{31}P NMR spectra obtained for the P1000 lignin are illustrated in Fig. 4. Several functions in the lignin structure were identified according to previous literature works [41,42]. For instance the presence of carboxylic acids was detected by ^{1}H NMR (12.3 ppm), by ^{13}C NMR (175–180 ppm) and by ^{31}P after phosphitylation (134 ppm). Similarly, methoxy groups were detected by ^{13}C

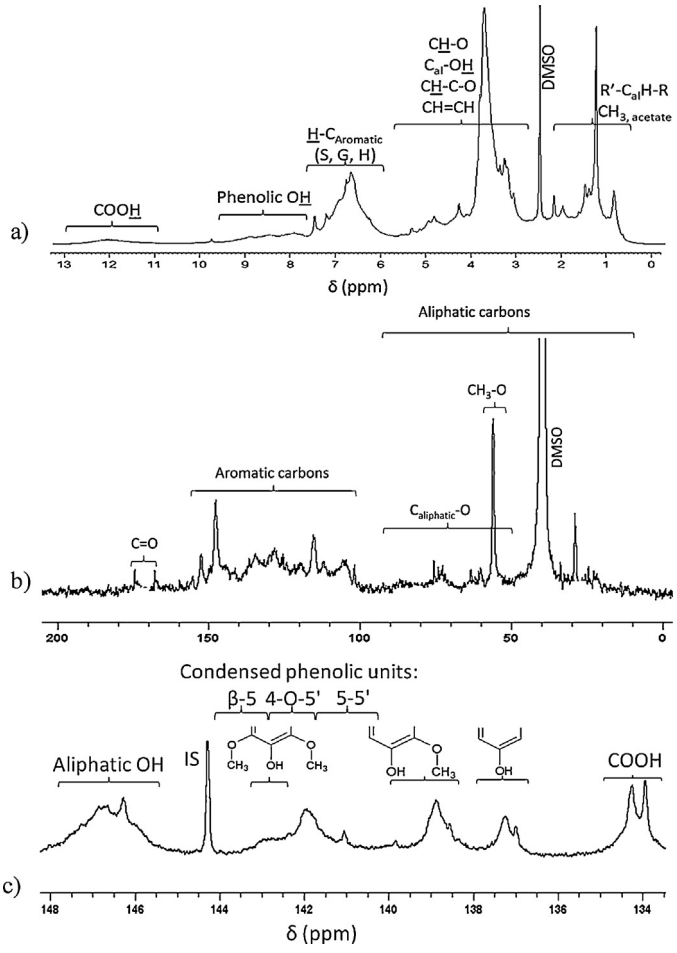

Fig. 4. (a) ^{1}H NMR, (b) ^{13}C NMR and (c) ^{31}P NMR spectra after phosphitylation of P1000 lignin.

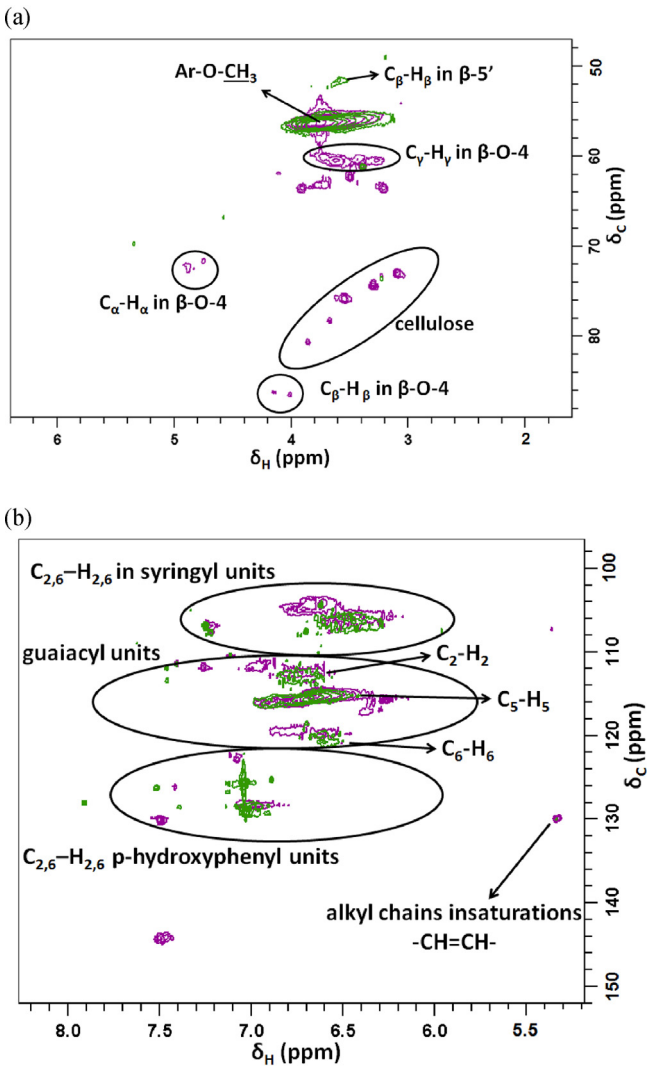

Fig. 5. HSQC spectra of the "oxygenated region" (a) and of the "aromatic region" (b) of initial lignin (purple) and the residue of lignin obtained at t_0 (green). (For interpretation of the references to color in this figure legend, the reader is referred to the web version of the article.)

(56 ppm) while ^{31}P NMR after phosphitylation allowed to distinguish these methoxy groups through the signals of guaiacyl and syringyl units (respectively 139 and 142.7 ppm). After attribution of the different peaks, a semi-quantification of the various typical groups relatively to the total hydrogen and carbon atoms was obtained for ^{1}H and ^{13}C (Tables 2 and 3) and an absolute quantification with ^{31}P NMR for the hydroxyl groups (Table 4). The molar ratio syringyl (S)/guaiacyl (G)/hydroxyphenyl (H) of P1000 lignin was about 48(S)/35(G)/17(H) as compared to values reported in the literature for wheat straw lignin extracted by mild alkaline hydrolysis 51.8(S)/44.5(G)/3.7(H) [43]. However, the proportion of syringyl groups is overestimated due to the signals of condensed phenolic units in the same region [36,37]. The HSQC NMR spectra (Fig. 5 and Table S3) indicate the presence of cellulosic and hemicellulosic residues, unsaturated aliphatic C—C and aliphatic C—H in β–β or β-O-4 linkages in addition of the syringyl, guaiacyl, hydroxyphenyl groups [44–46].

The GPC distribution of molar weights of the acetylated P1000 lignin is given in Fig. 6. The distribution is bimodal and the average molar weight is 4915 g mol^{-1} in polystyrene (PS) equivalent with a polydispersity of 3.1. This value corresponds to

Table 2
Relative quantification by ^{1}H NMR.

Groups	Chemical shift (ppm)	% integration		
		P1000 lignin	Lignin residue (with catalyst t_0)	Lignin residue (with catalyst 5 h)
Aliphatic H	0.6–2.3	24.0	22.9	31.0
Aromatic H	6.0–7.7	19.6	21.8	16.8
Phenolic OH	7.8–9.6	5.5	9.3	12.2
Carboxylic COOH	11.8–12.8	2.1	0.6	1.7
CH—CO, CH—O, Cal—OH	n.d.	48.8	45.4	38.3

Table 3
Relative quantification by ^{13}C NMR of P1000 lignin.

Groups	Chemical shift (ppm)	% integration
$C_{aliphatic}$(all included)	10–90	33
Methoxy CH_3—O	55	11
$C_{aliphatic}$—O (including O-CH_3)	50–90	24
$C_{aromatic}$	100–155	63
C=O	175–180	4

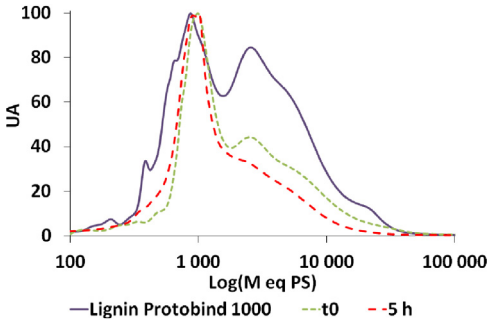

Fig. 6. GPC distribution of molar weights of P1000 lignin and lignin residues at t_0 and after 5 h of residence time.

approximately 27 phenylpropane units (the chosen standard unit is the hydroxypropyl-guaiacol $M = 178\ g\ mol^{-1}$).

These characterizations are in adequation with the type of lignin used [40], and will be helpful to discuss the primary stages of lignin hydroliquefaction.

3.2. Hydroconversion experiments: experimental product recovery protocol

In order to recover all the different gaseous, liquid and solid fractions after each experiment, the protocol described in Section 2 (Fig. 2) has been systematically implemented. This protocol allowed us to separate and analyze gases, THF-insolubles, THF-solubles and liquids with an excellent mass balance reaching 98%.

3.3. Characterization of the products after reaching the reaction temperature (t_0) with catalyst

When the experiment was stopped after reaching the reaction temperature (350 °C) the lignin conversion reached 27 wt% and products were composed of 3 wt% of gases, 24 wt% of liquids and 65 wt% of lignin residue (Fig. 7). We noted also that the THF-insolubles represent 8 wt%.

The THF-insolubles are still containing non-converted initial lignin. The gases are composed of methane (0.15 wt% of the initial lignin) and carbon dioxide (2.45 wt%). As can be seen in Fig. 8, light hydrocarbons (from C_2 to C_5) and carbon monoxide were also detected (0.03 wt% and 0.11 wt% of the initial lignin respectively). The presence of CO_2 suggests a decarboxylation stage and can be mainly attributed to the presence of carboxylic groups in the lignin. Indeed, the concentration of carboxylic acids determined

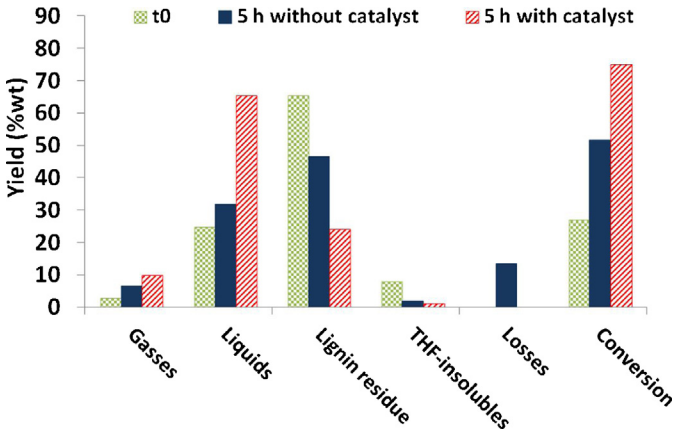

Fig. 7. Distribution of lignin hydroconversion products and conversion yield at t_0, and with and without NiMo catalyst (5 h residence time).

by ^{31}P NMR (Table 4) was much lower in the lignin residue when compared to Protobind 1000 lignin.

The THF-solubles fraction, solid at room temperature, is composed of residual lignin which is the partially cleaved and converted initial lignin, but still being an oligomeric entity. In order to evaluate the extent of conversion, this fraction was analyzed by the same techniques used for the characterization of the initial lignin. By comparison of the FTIR spectra, the lignin residue seems to be very similar to the initial lignin (Fig. 3). However, the GPC analysis illustrated by Fig. 6 evidenced that the lignin residue at t_0 presents a lower molecular weight distribution compared to the initial lignin. The distribution is still bimodal with an average molar weight is $3575\ g\ mol^{-1}$ in PS equivalent which corresponds to approximately 20 phenylpropane units and the polydispersity has decreased from 3.1 to 2.8.

The ^{1}H and ^{31}P NMR experiments carried out on lignin residue (Tables 2 and 4) indicate an increase of the amount of phenolic functions, but also a decrease of the amount of carboxylic and

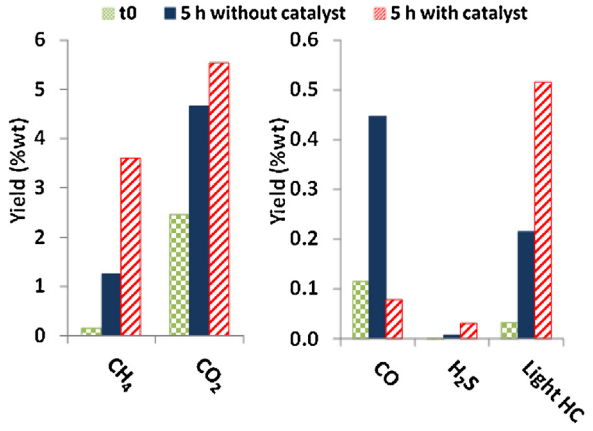

Fig. 8. Gaseous products composition at t_0, after 5 h without and with NiMo catalyst.

Table 4
Quantification by ^{31}P NMR after phosphitylation of P1000 lignin and lignin residues after t_0 and 5 h with catalyst.

Groups	Chemical shift (ppm)	Concentration (mmol OH/g of lignin or lignin residue)		
		Lignin P1000	Lignin residue t_0	Lignin residue 5 h
Aliphatic OH group	150.8–146.3	1.6	0.3	0.0
Syringyl phenolic units + condensed phenolic units	144.3–140.2	1.1	1.2	0.6
Guaiacyl phenolic units	140.2–138.4	0.8	0.7	0.3
p-Hydroxyphenolic units	138.6–136.9	0.4	0.8	1.9
Carboxylic COOH	135.6–133.7	0.9	0.2	0.2

aliphatic hydroxyl groups. Furthermore the HSQC experiments (Fig. 5) evidenced that the lignin residue at t_0 results from many transformations occurred on the initial lignin. For instance in Fig. 5a, we can observe the disappearance of the signals corresponding to Cα—Hα, Cβ—Hβ, Cγ—Hγ in β-O-4 linkages, and cellulose remaining fragments, as well as the decrease of methoxy groups present on aromatic rings and the formation of new Cβ—Hβ bonds corresponding to β-5 linkages (Fig. 1). The appearance of such linkages at this stage suggests favorable conditions for intramolecular cyclization reactions leading to cyclic ether. As illustrated in Fig. 5b, the contribution of syringyl units was clearly lower as compared to the initial lignin, while guaiacyl and hydroxyphenyl units became more important. This figure also indicates the disappearance of double bonds in aliphatic chains (5.5/130 ppm) and in Cα (7.5/144 ppm).

Moreover, molecular composition of the liquid phase was investigated by comprehensive two-dimensional chromatography GC × GC–MS. This powerful technique provides a detailed description of the products [47]. The following chemical families were detected in liquid fractions: dimethoxyphenols, methoxyphenols, phenols, aromatics, alkanes, naphthenes. We can then observe that after reaching the reaction temperature (t_0), alkyldimethoxyphenols and alkylmethoxyphenols are present in the liquid phase with a few alkylphenols, aromatics, alkanes (C_{13}–C_{18}) and naphthenes (Fig. 12a). A C_{18} fatty acid with two unsaturations was also detected in the liquid phase. This linoleic acid (and possibly other type of fatty acids not yet detected) probably comes from the wheat grain and remains after the pretreatment and can be the precursor of detected alkanes.

To summarize, by heating the initial lignin up to 350 °C under H_2 and in the presence of tetralin and a NiMo catalyst, structural modifications of the Protobind lignin occurred leading to the formation of a t_0 lignin residue having a different chemical composition. Molecular analysis of the liquid products indicated that monomeric phenols have been formed while basic transformations like dehydroxylation, dehydration, demethylation or decarboxylation occurred in some extent leading to shorter lignin fragments.

3.4. Conversion without catalyst after 5 h of residence time

An experiment has been carried out in thermal conditions without catalyst but in the presence of hydrogen and tetralin, in order to evaluate properly the effect of the catalyst after a residence time of 5 h. In such operating conditions, the lignin conversion only reached 52 wt% (including 12.6 wt% losses supposed to be liquid products, see Fig. 9). Effectively the experiment was repeated several times with still a high level of losses. No explanation has been found but it is reasonable to think that these losses are liquids, probably mainly water. However, the distribution of products varied drastically as compared to the catalytic experiment also performed for a 5 h residence time (Fig. 9). The liquid yield was low (32 wt%) while the lignin residue (THF-solubles) reached 47 wt% and THF-insolubles 2 wt%. The H/C atomic ratio of the lignin residue (THF-solubles) was lower than the H/C ratios obtained in the presence of catalyst (t_0 and t = 5 h). The lignin residue obtained without catalyst was thus less hydrogenated compared to the residues recovered after the

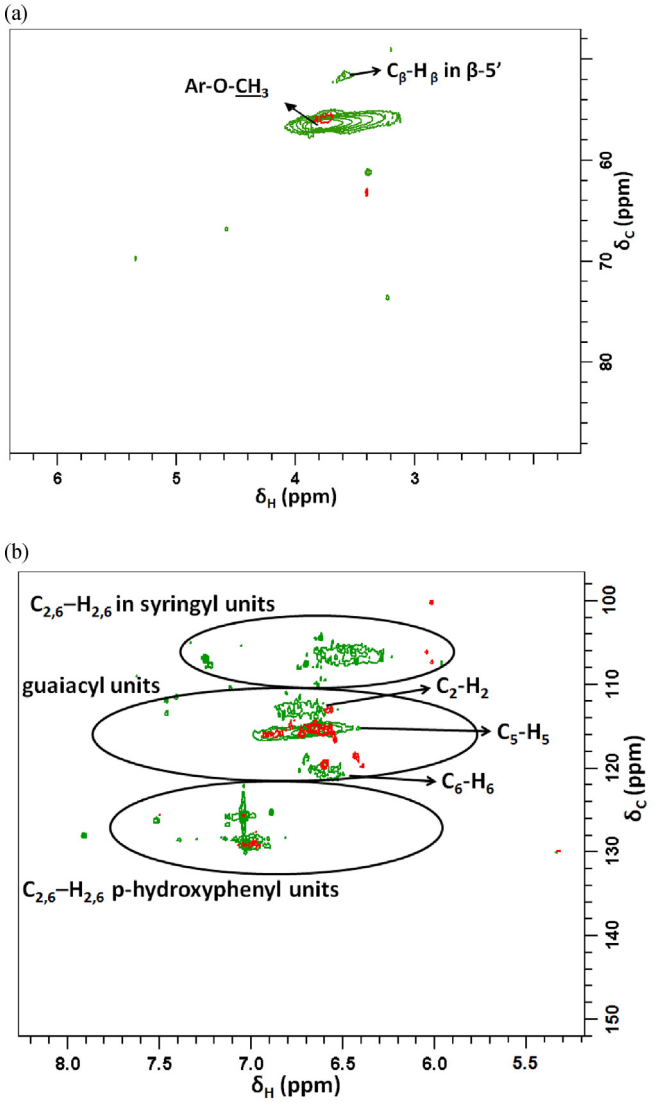

Fig. 9. HSQC spectra of the "oxygenated region" (a) and of the "aromatic region" (b) of the residue of lignin obtained at t_0 (green) and the residue of lignin obtained after 5 h of reaction (red). (For interpretation of the references to color in this figure legend, the reader is referred to the web version of the article.)

catalytic experiments. On the other hand, the O/C atomic ratio was decreased compared to the t_0 experiment but was identical after 5 h of residence time with and without catalyst. The gases (7 wt%) were mainly composed of CO_2 (4.7 wt%) and also CH_4 (1.25 wt%), CO (0.45 wt%) and lights alkanes (0.21 wt%) (Fig. 7). A larger contribution of CO is noticed as compared to the catalytic experiments where CO_2 is the major gas product indicating the occurrence of water gas shift reaction. The 2D-GC chromatogram obtained from the liquid (not shown) indicated the presence of dimethoxy and methoxyphenols as the main compounds and a few alkylphenols, aromatics, alkanes and naphthenes.

3.5. Hydroliquefaction experiment at 5 h residence time with catalyst

After a residence time of 5 h, the ash-free conversion of lignin reached 75 wt%, with the following yields: 9.8 wt% of gases, 65.4 wt% of liquids, 24 wt% of THF-solubles. The solid recovered (THF-insolubles), after Soxhlet extraction, was composed of solid lignin residue, ashes and catalyst. The catalyst extrudates were not damaged during the experiment and were easily removed. Finally, the solid lignin residue represent only 1 wt% of the initial lignin.

3.5.1. Characterization of the used catalyst

In order to evaluate the coke formation during the reaction, TPO experiments (not shown) were undertaken with the used catalyst. These experiments coupled with the CHONS analyses, indicated that coke was formed during the experiment characterized by an oxidation peak between 300 and 580 °C. After the reaction, sulfur content of the catalyst decreases to 7 wt% (corrected from C content) versus 9 wt% in its freshly sulfided state and the carbon content reached 11 wt%.

3.5.2. Characterization of gases

The μGC–TCD–MS analysis of the gases, which productivity reached 9.8 wt% of the initial lignin, indicated that methane and carbon dioxide were the major components (3.6 wt% and 5.5 wt% of the initial lignin respectively). Light alkanes from C_2 to C_5 and carbon monoxide (0.52 wt% and 0.07 wt% respectively) were also detected (Fig. 7). Compared to t_0 data, the production of CO_2 is more than twice higher. In addition, a large enhancement in the production of CH_4 was measured. CH_4 originated either from the hydrogenation of the cleaved methoxy or methyl groups from guaiacyl and syringyl units and/or from carbon oxides methanation. Compared to the thermal experiment without catalyst, the presence of the catalyst had an effect on the gases selectivity since there is a simultaneous increase in the amount of CO_2 and CH_4 in the presence of the catalyst. Both water gas shift and methanation catalytic reactions occur under our experimental operating conditions leading to CO_2 and CH_4 [48] and the presence of the catalyst allowed these processes to occur contrarily to the experiment done without catalyst.

3.5.3. Characterization of the lignin residue

After a residence time of 5 h with NiMo catalyst, the recovered THF-solubles fraction represented 24 wt% of the initial lignin. From GPC analysis (Fig. 6), we observed that the distribution of molar weights of residual lignin obtained after 5 h of reaction was similar to the lignin residue at t_0, with, however, a lower polydispersity (2.4) and a shortening of the longer entities. We note also that some chains centered around 800 g mol^{-1} polystyrene (PS) equivalent were transformed. The average molecular weight of the residual lignin is 2303 g mol^{-1} PS eq. which could be represented by 13 units as compared to 27 units for the initial lignin and 20 units for the t_0 lignin residue.

By elemental analyses, we observed that the H/C atomic ratio decreased slightly from 1.12 to 0.97 while the O/C ratio dramatically decreased from 0.32 to 0.11. This trend evidenced the deoxygenation of the residual lignin mostly by ether and hydroxyl bonds cleavage.

The FTIR spectra of residual lignin showed the decrease of C=O bonds corresponding to carboxylic acids (1700–1715 cm^{-1}), the decrease of the intensities syringyl (1334 and 1125 cm^{-1}) and guaiacyl (1183 and 838 cm^{-1}) units and the decrease of hydroxyl aliphatic groups (1090 cm^{-1}). ^{31}P NMR experiments after phosphitylation evidenced the disappearance of aliphatic and carboxylic OH groups and the decrease of syringyl and guaiacyl groups while hydrophenyl units increased. This is the result of the progressive removing of methoxy groups in the lignin structure. HSQC experiments confirmed this result since for the C—H aromatic region (Fig. 9b) only guaiacyl and hydroxyphenyl units remained after 5 h of reaction. In Fig. 9a, we can observe the continuous decrease of methoxy groups on aromatic rings and the disappearance Cβ—Hβ in β–β linkages formed at t_0. Furthermore, in the aliphatic region (C: 15–30 ppm, H: 0.8–1.4 ppm), we observed (not shown) that aliphatic chains (CH_3, CH_2) were still present and the signals were even more intense in lignin residue. Thus, we can propose that the cyclic ether in β–β and β-5 bond types were converted into aliphatic chains linking two aromatic rings as illustrated in Fig. 10.

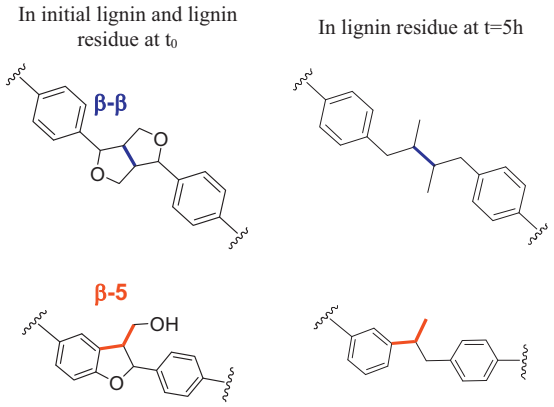

Fig. 10. Illustration of the transformation of β–β and β-5 linkages in lignin and lignin residues during catalytic step.

Finally, this lignin residue is a shorter lignin containing around 14 units instead of 27 at the beginning, which has been deoxygenated. Several processes were identified after 5 h of conversion:

- The dehydroxylation of the aliphatic OH groups leading to formation of water.
- The decarboxylation of carboxylic acids functions with formation of CO_2.
- The saturation of aliphatic double bonds.
- The demethoxylation of syringyl units to guaiacyl and then to hydroxyphenyl.
- The ether linkages cleavage which deliver phenols in the liquid phase.

The early stage of hydroconversion (up to t_0) allowed to break the weakest linkages (β-O-4, -OMe, -OH) of the lignin and to convert β–β and β-5. Fig. 10 presents the transformation occurring for the β–β and β-5 linkages in our operating conditions. These linkages are few compared to β-O-4 which cleavage gave phenols, but the presence of those explain why after 5 h lignin residue is still presenting oligomeric chains but without the initial β-O-4, β–β, β-5 linkages. Apparently after 5 h of residence time, some of the linkages broken are of the same type of the ones cleaved after reaching the reaction temperature but of course they are many in comparison, we also observed the deep improvement of the cleavage of $C_{aromatic}$—OMe (HSQC) which convert syringyl to guaiacyl and then to phenolic. The further catalytic stage extended the cleavage by transforming all the cyclic ether into aliphatic bridging chains. After 5 h, the relative size of the lignin (or lignin residue) was reduced by a factor of two. Undoubtedly, the lignin residue still contains some stronger C—C linkages which will be more difficult to cleave. A tentative structure for the lignin residue after 5 h of conversion is proposed to illustrate the different trends observed on this material especially by HSQC NMR: presence of saturated alkylchains, aromatics, and some phenolic and methoxy groups (Fig. 11).

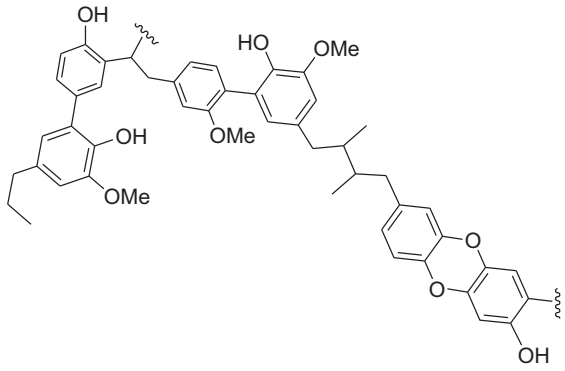

Fig. 11. Example of possible structure of lignin residue after 5 h of residence time.

3.5.4. Characterization of the liquid phase

The liquid phase, which represents 65.4 wt% of the initial lignin, is the most difficult fraction to characterize, not only because of the complexity of the mixture but also because of the presence of the tetralin solvent. The amount of tetralin in the solution (i.e. 84 wt%) was determined using gas chromatography and standard addition method. While the reaction proceeds, water was formed and remained in the liquid fraction. Unfortunately, the Karl–Fisher water analysis of the liquid fraction was not reproducible. Qualitative characterization of the liquid phase was obtained by 2D-GC–MS. The presence of the catalyst increased dramatically the concentration of phenols, aromatics and naphthenes in the liquid phase if we compare with the 2D-GC chromatogram obtained for the 5 h experiment without catalyst (not shown). After 5 h of reaction with a NiMo catalyst, dimethoxyphenols disappeared, methoxyphenols decreased while phenols, aromatics, naphthenes and alkanes (C_{13}–C_{18}) became the major components (Fig. 12b). The nature of these compounds is in accordance with the transformations observed on the lignin residue. The dimethoxyphenols are readily formed by β-O-4 linkages cleavage at the end of the polymeric chains. Then, the demethoxylation occurred and lead to methoxyphenols and to alkylphenols, further converted by hydrodeoxygenation (HDO) to aromatics and naphthenes [28,49–51]. The presence of C_{13}–C_{18} alkanes in the liquid phase was quite surprising. One valid hypothesis is that these alkanes came from the deoxygenation of the fatty acids previously detected in the liquid phase. This assumption has to be confirmed and the quantification of liquid compounds is under investigation by using new techniques and procedures.

(a)

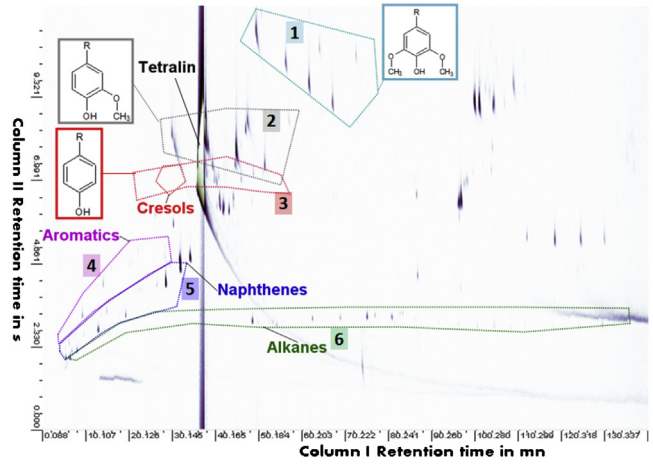

(b)

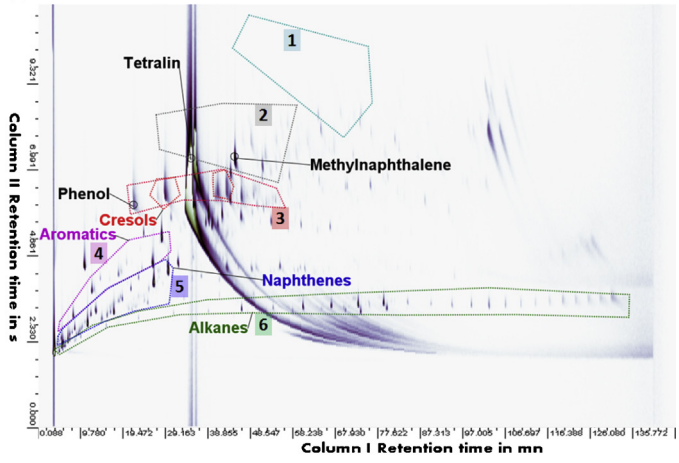

Fig. 12. 2D-GC–MS chromatogram of the bio-liquid obtained after (a) reaching the reaction temperature $t = t_0$ and (b) 5 h of reaction.

4. Conclusion

A wheat straw soda lignin (Protobind 1000) was taken as starting material to perform hydroconversion under H_2 and in the presence of tetralin with a sulfided NiMo catalyst on alumina in a batch reactor. The initial lignin was deeply characterized with advanced spectroscopic and chromatographic techniques in order to get the evolution of characteristic organic functions occurring during the conversion. Thanks to the developed experimental product recovery protocol we have been able to separate the different products after hydroconversion of lignin and to reach a very good mass balance of 98% (±3.5 wt%). From the analytical characterization of the different products, it was possible to investigate what kind of reactions already occurred when heating up the Protobind lignin at 350 °C (reaction stopped when the targeted temperature was reached). We showed that lignin was submitted to dehydroxylation, dehydration, demethylation or decarboxylation reactions during the 14 min reactor heating. Under our operating conditions, after a residence time of 5 h at 350 °C with NiMo catalyst, the lignin was converted into gases (9 wt%), liquids (65 wt%) and a lignin residue has been recovered and characterized. The lignin residue was already deeply transformed, one fraction of it being kept solubilized in the liquid product. The lignin residue contained shorter lignin-type fragments than the initial lignin and resulted from the transformation of Protobind 1000 lignin through several reactions (dehydroxylation, decarboxylation, demethoxylation, bonds saturation and cleavage). The liquids were a mixture of phenols, aromatics, naphthenes and alkanes. Considering the results obtained after a residence time of 5 h, longer experiments will be performed to reach even higher yield of liquids from lignin by converting further the lignin residue into liquid.

Acknowledgement

B. Joffres thanks IFP Energies nouvelles for a PhD grant.

Appendix A. Supplementary data

Supplementary data associated with this article can be found, in the online version, at http://dx.doi.org/10.1016/j.apcatb.2013.01.039.

References

[1] A. Abächerli, F. Doppenberg, Method for preparing alkaline solutions containing aromatic polymers, Patent PCT/IB98/00512, WO 98/42912 (1998), pp. 1–16.
[2] R.J.A. Gosselink, M.H.B. Snijder, A. Kranenbarg, E.R.P. Keijsers, E. de Jong, L.L. Stigsson, Industrial Crops and Products 20 (2004) 191–203.
[3] R.J.A. Gosselink, E. de Jong, B. Guran, A. Abächerli, Industrial Crops and Products 20 (2004) 121–129.
[4] P. Sannigrahi, Y. Pu, A. Ragauskas, Current Opinion in Environmental Sustainability 2 (2010) 383–393.
[5] W.D. Goheen, in: J. Marton (Ed.), Lignin Structure and Reactions, American Chemical Society, 1966, pp. 205–225.
[6] J.S. Shabtai, W.W. Zmierczak, E. Chornet, Process for conversion of lignin to reformulated, partially oxygenated gasoline, US 6172272 B1 (2001).
[7] D.T.A. Huibers, H.J. Parkhurst, Lignin hydrocracking process to produce phenol and benzene, US 4420644 (1983).
[8] M. Kleinert, T. Barth, Chemical Engineering and Technology 31 (2008) 736–745.
[9] M. Kleinert, T. Barth, One-step conversion of solid lignin to liquid products, EP 2025735 A1 (2009).
[10] D.R. Dimmel, in: C. Heitner, D.R. Dimmel, J.A. Schmidt (Eds.), Lignin and Lignans: Advances in Chemistry, CRC Press, Boca Raton, USA, 2010, pp. 1–10.
[11] J. Zakzeski, P.C.A. Bruijnincx, A.L. Jongerius, B.M. Weckhuysen, Chemical Reviews 110 (2010) 3552–3599.
[12] D.R. Dimmel, G. Gellerstedt, in: C. Heitner, D.R. Dimmel, J.A. Schmidt (Eds.), Lignin and Lignans: Advances in Chemistry, CRC Press, Boca Raton, USA, 2010, pp. 349–392.
[13] C. Arato, E.K. Pye, G. Gjennestad, Applied Biochemistry and Biotechnology 121–124 (2005) 871–882.
[14] L. da Costa Sousa, S.P.S. Chundawat, V. Balan, B.E. Dale, Environmental Biotechnology 20 (2009) 339–347.
[15] W.G. Glasser, R.S. Wright, Biomass and Bioenergy 14 (1998) 219–235.
[16] C. Amen-Chen, H. Pakdel, C. Roy, Bioresource Technology 79 (2001) 277–299.
[17] P. de Wild, R.V. der Laan, A. Kloekhorst, E. Heeres, Environmental Progress and Sustainable Energy 28 (2009) 461–469.
[18] D.J. Nowakowski, A.V. Bridgwater, D.C. Elliott, D. Meier, P. de Wild, Journal of Analytical and Applied Pyrolysis 88 (2010) 53–72.
[19] P. de Wild, W.J.J. Huijgen, H.J. Heeres, Journal of Analytical and Applied Pyrolysis 93 (2012) 95–103.
[20] X. Wang, R. Rinaldi, ChemSusChem 5 (2012) 1455–1466.
[21] N.P. Vasilakos, D.M. Austgen, Industrial and Engineering Chemistry Process Design and Development 24 (1985) 304–311.
[22] D.F. McMillen, R. Malhotra, D.S. Tse, Energy and Fuels 5 (1991) 179–187.
[23] K. Kidena, N. Bandoh, M. Kouchi, S. Murata, N. Nomura, Fuel 79 (2000) 317–322.
[24] H.E. Jegers, M.T. Klein, Industrial and Engineering Chemistry Process Design and Development 24 (1985) 173–183.
[25] A. Vuori, J.B.-son Bredenberg, Holzforschung 42 (1988) 155–161.
[26] R. Thring, J. Breau, Fuel 75 (1996) 795–800.
[27] A. Oasmaa, R. Alén, D. Meier, Bioresource Technology 45 (1993) 189–194.
[28] W.J. Connors, L.N. Johanson, K.V. Sarkanen, P. Winslow, Holzforschung 34 (1980) 29–37.
[29] O. Faix, J. Bremer, D. Meier, I. Fortmann, M.A. Scheijen, J.J. Boon, Journal of Analytical and Applied Pyrolysis 22 (1992) 239–259.
[30] D. Meier, C. Grünwald, O. Faix, Journal of Analytical and Applied Pyrolysis 25 (1993) 335–347;
D. Meier, O. Faix, Biomass and Bioenergy 7 (1994) 99–105.
[31] G.P. Curran, R.T. Struck, E. Gorin, Industrial and Engineering Chemistry Process Design and Development 6 (1967) 166–173.
[32] K. Marchand, C. Legens, D. Guillaume, P. Raybaud, Oil and Gas Science Technology 64 (6) (2009) 719–730.
[33] B. Cathala, B. Saake, O. Faix, B. Monties, Journal of Chromatography A 1020 (2003) 229–239.
[34] M.E. Himmel, J. Mlynar, S. Sarkanen, in: C. Wu (Ed.), Handbook of Size Exclusion Chromatography, Marcel Dekker, New York, 1995, pp. 353–379.
[35] T.A. Milne, H.L. Chum, F. Agblevor, D.K. Johnson, Biomass and Bioenergy 2 (1992) 341–366.
[36] D.S. Argyropoulos, Journal of Wood Chemistry and Technology 13 (2) (1993) 187–212.
[37] A. Granata, D.S. Argyropoulos, Journal of Agricultural and Food Chemistry 43 (1995) 1538–1544.
[38] J. Stihle, D. Uzio, C. Lorentz, N. Charon, J. Ponthus, C. Geantet, Fuel 95 (2012) 79–87.
[39] S.Y. Lin, C.W. Dence (Eds.), Methods in Lignin Chemistry, Springer-Verlag, Heidelberg, 1992.
[40] U.P. Agarwal, R.H. Atalla, in: C. Heitner, D.R. Dimmel, J.A. Schmidt (Eds.), Lignin and Lignans: Advances in Chemistry, Taylor and Francis, 2010, pp. 103–136.
[41] J. Ralph, L.L. Landucci, in: C. Heitner, D.R. Dimmel, J.A. Schmidt (Eds.), Lignin and Lignans: Advances in Chemistry, Taylor and Francis, 2010, pp. 137–244.
[42] C. Crestini, G.G. Sermanni, D.S. Argyropoulos, Bioorganic and Medicinal Chemistry 6 (1998) 967–973.
[43] C. Lapierre, in: C. Heitner, D.R. Dimmel, J.A. Schmidt (Eds.), Lignin and Lignans: Advances in Chemistry, Taylor and Francis, 2010, pp. 11–48.
[44] S.-N. Sun, M.-F. Li, T.-Q. Yuan, F. Xu, R.-C. Sun, Industrial Crops and Products 37 (2012) 51–60.
[45] J. Zakzeski, A.L. Jongerius, P.C.A. Bruijnincx, B.M. Weckhuysen, ChemSusChem 5 (2012) 1602–1609.
[46] http://afrsweb.usda.gov/SP2UserFiles/Place/36553000/software/NMR/NMR_DB_11-2004.pdf, U.S. Department of Agriculture.
[47] X. Wang, R. Rinaldi, Energy and Environmental Science 5 (2012) 8244–8260.
[48] A. Pineihro, N. Dupassieux, D. Hudebine, C. Geantet, Energy and Fuels 23 (2009) 1007–1014.
[49] C. Bouvier, Y. Romero, F. Richard, S. Brunet, Green Chemistry 13 (2011) 2441–2451.
[50] V.N. Bui, D. Laurenti, P. Delichère, C. Geantet, Applied Catalysis B: Environmental 101 (2011) 246–255.
[51] J. Horacek, F. Homola, I. Kubickova, D. Kubicka, Catalysis Today 179 (2012) 191–198.